Improved Fluorescence of Carbon Dots Prepared from Bagasse under Alkaline Hydrothermal Conditions

Xiao-Juan Liu,[a] Ming-Lin Guo,[b],* Juan Huang,[b] and Xue-Yan Yin [a]

A simple and effective route to improve the fluorescence of carbon dots is reported. A weak fluorescent solution was obtained by a diminution step to obtain tiny particles from bagasse-based carbonaceous blocks. This solution was subjected to hydrothermal treatment under alkaline conditions to improve its fluorescent performance. The luminescence was found to be improved by more than 20-fold after hydrothermal treatment. The ultraviolet absorption and the surface structure were also significantly changed. The alkaline hydrothermal process was shown to involves hydrolysis, isomerization, dehydration, and polymerization that causes the formation of the C=C double bonds and conjugated structures. The optimum hydrothermal conditions were at 200 °C for 8 h, and the most appropriate ratio of NaOH to the amount of the weak fluorescent solution was 38-40 mg to 1 mL.

Keywords: Fluorescent carbon dots; Bagasse; Sodium hydroxide; Hydrothermal

*Contact information: a: Department of Materials, Tianjin Polytechnic University, Tianjin 300387, China; b: Department of Environment and Chemical Engineering, and Key Laboratory of Hollow Fiber Membrane Materials and Membrane Process, Tianjin Polytechnic University, Tianjin 300387, China; *Corresponding author: guomlin@yahoo.com*

INTRODUCTION

Carbon dots (CDs) can be used in the fields of cellular imaging, biosensing, and drug delivery because of the superior advantages in the chemical stability and biological compatibility in comparison to the traditional semiconductor quantum dots. Many researchers have developed a variety of synthetic methods to prepare environment-friendly CDs, including laser irradiation of graphite (Sun *et al*. 2006; Hu *et al*. 2009), electrochemical oxidation of graphite (Zhao *et al*. 2008; Zheng *et al*. 2009), multi-walled carbon nanotubes (Zhou *et al*. 2007), neutron beam radiation of nano-diamond (Yu *et al*. 2005; Fu *et al*. 2007), chemical oxidation (Liu *et al*. 2007; Tian *et al*. 2009; Peng and Travas-Sejdic 2009; Liu *et al*. 2009; Ray *et al*. 2009; Zhang *et al*. 2010; Pan *et al*. 2010;), hydrothermal oxidation (Bourlinos *et al*. 2008) of the appropriate precursors, and microwave decomposition of carbohydrates (Zhu *et al*. 2009).

The production of CDs usually has utilized surface modification to enhance the fluorescent intensity. Typically, nitric acid oxidative treatment has been used to introduce carbonyl functionalities at the surfaces (Liu *et al*. 2007; Tian *et al*. 2009; Dong *et al*. 2010), and different surface passivate agents, primarily amino-terminated reagents, have been then used for the surface passivation of CDs through the formation of amide linkages (Peng *et al*. 2009; Liu *et al*. 2009). These methods can improve the quantum yields about 10-fold. In addition, Tian *et al.* (2010) improved the photoluminescence more than 10-fold by removal of quinine moieties under neutral hydrothermal conditions. However, little effort had been made to enhance the fluorescence under alkaline hydrothermal conditions. This method was found to be quite different from the existing methods. The structure and the fluorescence was completely changed after alkaline hydrothermal treatment, with the quantum yield increased by 20-fold. This method is entirely novel and significantly more effective.

Biomass is widely used as a carbon source because of its sustainability. Bagasse is considered to be an important biomass waste due to its cheap price and renewability. Bagasse-based carbonaceous blocks were used for this study. First, the bagasse material was soaked in concentrated sulfuric acid for 24 h at room temperature so as to obtain the carbonaceous blocks (Fig. 1). Second, the carbonaceous blocks were treated using an aqueous solution of sodium hydroxide (NaOH) at reflux temperature. The filtrate from the reflux system was a dark solution (designated as S-A), but its fluorescence was relatively weak, with the quantum yield of 0.2% under the 330 nm excitation wavelength. Finally, an alkaline hydrothermal treatment was performed on the S-A. A bright yellow solution (designed as S-B) was obtained. The quantum yield of this solution rose to 4.7%.

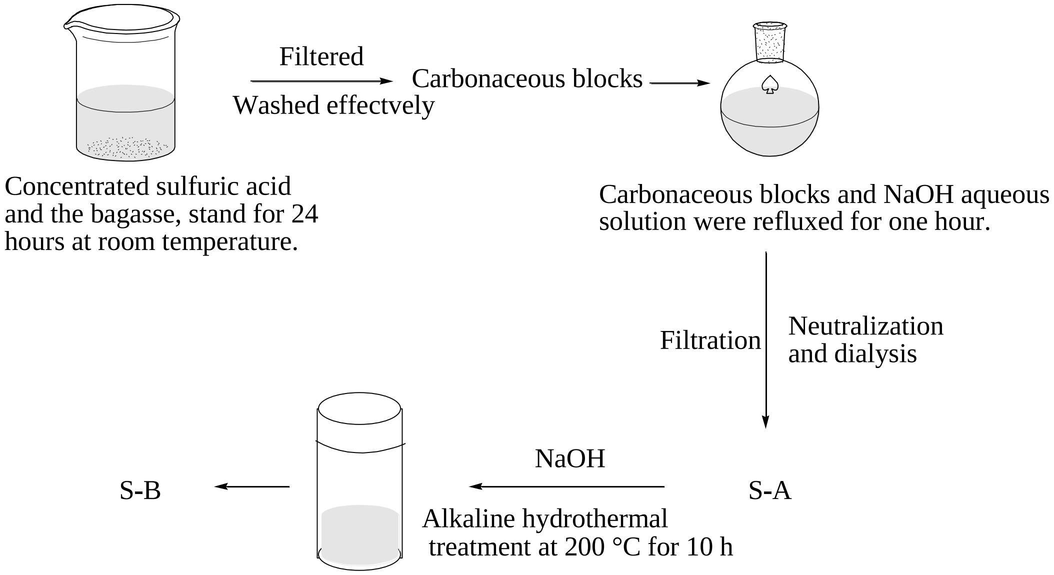

Fig. 1. The experimental procedures of this article. Step I: The mixture of concentrated sulfuric acid and the bagasse stood for 24 h at room temperature. Then the carbonaceous blocks were obtained by effectively washing the solid mixture. Step II: Carbonaceous blocks and NaOH aqueous solution were refluxed for one hour. The filtrate from the reflux system was designated as S-A after neutralization and dialysis. Step III: The S-A was subjected to an alkaline hydrothermal treatment at 200 °C for 10 h, the resulting solution was designated as S-B.

We conducted detailed ultraviolet-visible (UV-vis) and fluorescence spectra, X-ray photoelectron spectroscopy (XPS), and transmission electron microscopy (TEM) studies to further elucidate the physical-chemical processes involved in the transformation of the structure and the properties. Based on the obtained experimental evidence, it was established that the alkaline hydrothermal process involves hydrolysis, isomerization, dehydration, and polymerization, causing the formation of the C=C double bonds and conjugated structures.

EXPERIMENTAL

In a typical process, 5 g of bagasse and 10 mL of concentrated sulfuric acid (98 wt.%) were fully mixed by stirring and were kept for 24 h at room temperature. Then, the solid was washed repeatedly with hot water and alcohol until the filtrate was neutral and dried in an oven at 80 °C overnight to obtain the carbonaceous blocks. A mixture of 0.2 g of the carbonaceous blocks and 100 mL of 0.025 mol / L NaOH were refluxed for one hour, followed by filtering to remove the large particles. The filtrate was neutralized and dialyzed against water through a dialysis membrane (MWCO 3500) for 24 h to obtain the S-A. The solid content of S-A was 1.8 mg/mL. Its fluorescence was weak. Then, a mixture of 2 mL of the S-A, 8 mL of water, and 114 mg of NaOH were sealed into a typical polytetrafluoroethylene-lined (PTFE-lined) autoclave system and hydrothermally reacted in a pre-heated oven at 200 °C for 10 h. The product was then neutralized with chlorhydric acid and dialyzed against water through the dialysis membrane for 24 h. This method finally allowed the S-B to be obtained. The solid content of S-B was 0.5 mg/mL.

The UV-vis absorption spectra were recorded on a UV-1901 spectrophotometer between 200 and 700 nm at room temperature. XPS analysis was measured on an EDAX GENESIS 60S spectrometer using Mg as the exciting source. The fluorescent spectra of the complex were measured on a Gangdong F-380 fluorescence spectrometer. TEM images were observed by a Hitachi H-7650 microscopy.

Quantum yield was measured according to established procedure (Lakowicz 1999). Quinine sulfate in 0.1 M H_2SO_4 (quantum yield 0.54 at 370 nm) was chosen as a standard. Absolute values were calculated using the standard reference sample that has a fixed and known fluorescence quantum yield value, according to the following equation,

$$\varphi_x = \varphi_{std} \frac{I_x}{A_x} \frac{A_{std}}{I_{std}} \frac{\eta_x^2}{\eta_{std}^2} \tag{1}$$

where φ is the quantum yield, I is the measured integrated emission intensity, A is the optical density, and η is the refractive index. The subscript "std" refers to the reference fluorescence of known quantum yield. An excitation slit width of 5 nm and an emission slit width of 5 nm were used to excite the samples and to record their photoluminescence spectra.

RESULTS AND DISCUSSION

The fluorescence of S-A was very weak with the quantum yield of 0.2% under a 330 nm excitation wavelength. The S-B had strong fluorescence. The quantum yield was 4.7%, with a maximum emission spectrum at 420 nm under 330 nm excitation wavelengths (Fig. 2a). Photographs of S-A and S-B under ambient light and ultraviolet light (365 nm) are shown in Fig. 2b. As seen from Fig. 2b, the S-B had an obviously stronger blue color than the S-A, revealing that the fluorescence had been significantly improved.

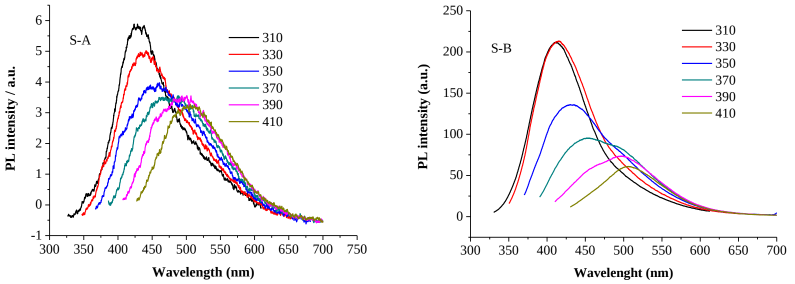

Fig. 2. (a) Emission spectra of the S-A and the S-B at different excitation wavelengths progressively increased from 310 nm with a 20 nm increment.

(b)

Fig. 2. (b) The photographs of S-A and S-B under ambient light and ultraviolet light (365 nm).

Figure 3a shows the UV-vis spectra of the S-A and the S-B. The spectrum of the S-B showed significant absorptions in the wavelength range of 200 to 300 nm rather than S-A. This revealed that the double bonds and conjugated structures (Kaczmarek and Czerwinski 2002) were rare in the S-A, but these structures were increased in the S-B by the basic hydrothermal reaction. Infrared spectroscopy (Fig. 3b) shows the S-B had a obvious broad band at 472 cm^{-1},which can be ascribed to graphitic domains (Bourlinos *et al*. 2012). The similar characteristic absorption bands at 3430 cm^{-1}, 1631 cm^{-1}, 1598 cm^{-1}, 1382 cm^{-1}, 1351 cm^{-1}, and 1105 cm^{-1} of the S-A and the S-B reveals a common origination from the hydroxyl group of alcohol or phenolorigin, C=O in p-substituted arylketones, C=C coupled with benzene ring, and C-O.

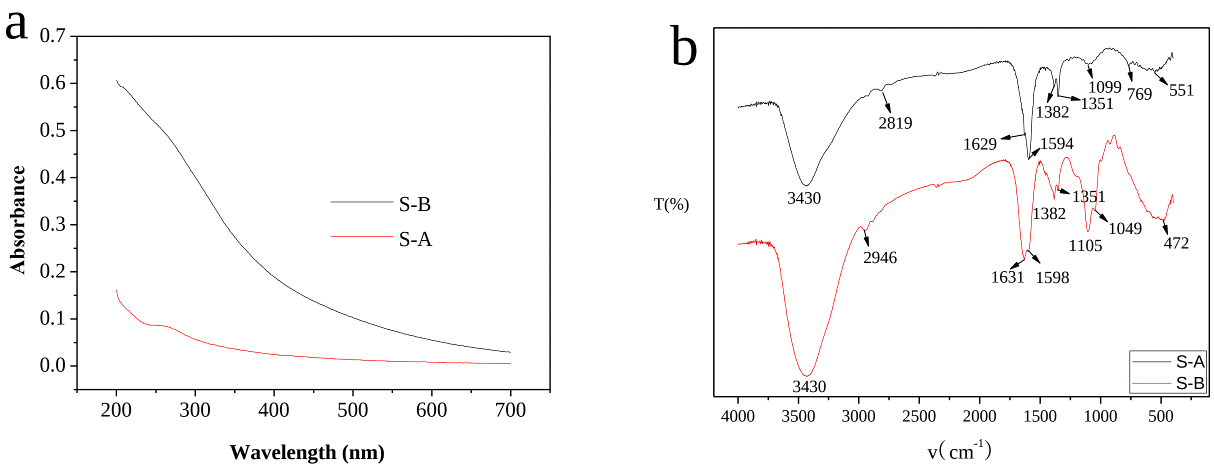

Fig. 3. UV-vis spectra and infrared spectroscopy of the S-A and S-B

The surface structures of the S-A and S-B were characterized by XPS techniques. As shown in Fig. S1 in the Appendix, both exhibited three strong peaks, which were respectively attributed to C1s, O1s, and Na1s.

The atomic ratios of the S-A were C - 51.14%, O - 32.24%, and Na - 6.91 % ($CO_{0.63}Na_{0.135}$), respectively, while the atomic ratios of the S-B were C - 64.97%, O - 23.6% and Na - 8.14% ($CO_{0.363}Na_{0.125}$), respectively, which revealed that the oxygenated groups on the surface of the S-A were significantly removed through hydrothermal treatment under alkaline conditions.

Furthermore, the C1s and the O1s fitting analysis for the S-A and S-B in Fig. 4 illustrate that the peak at 288 eV of carbon attributed to carboxyl groups on the surface of the S-B was significantly enhanced from 10.47% to 39.75%, while the peaks at 286 eV of C-O were significantly weakened from 45.74% to 17.03% after the hydrothermal reaction of the S-A (Zhou *et al*. 2007).

The O1s fitting analysis revealed a similar law. In addition, the ratios of the Na and O atoms of the S-B were 34.4%, which was higher than 21.5% of the S-A. All these discoveries suggested that there were more carboxyl groups on the surface of the S-B than that of the S-A.

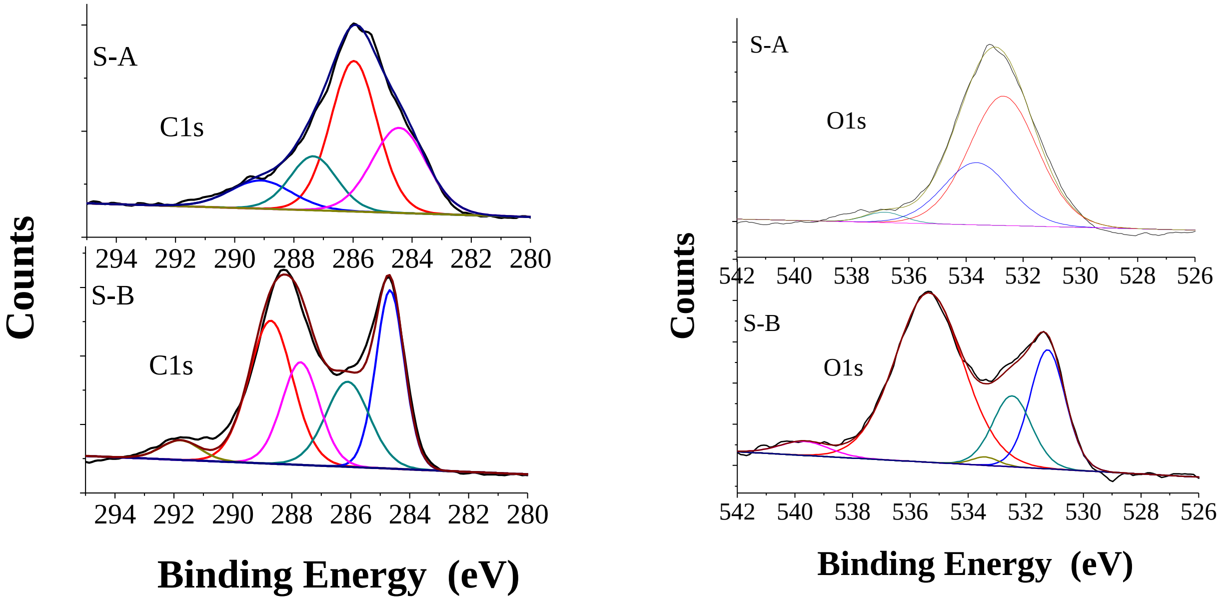

Fig. 4. XPS analysis of the C1s (a) and O1s (b) of the S-A and S-B

Figure 5 showed the TEM images of the S-A (a) and the S-B (b) and the size distribution analysis of them measured by Nano Measurer 1.2. It could be seen from Figure 5a that the S-A were nano dots with the average particle size of 5.18 nm. In Figure 5b, the monodisperse luminescent CDs with the average diameter of 2.94 nm were observed.

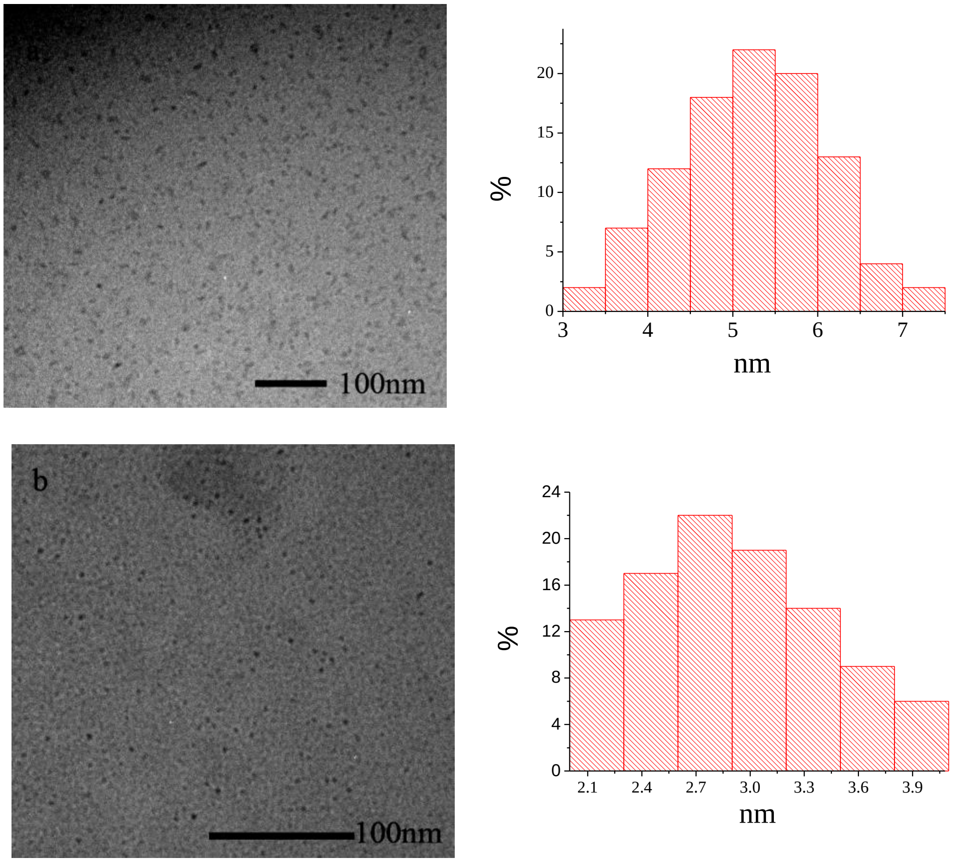

Fig. 5. TEM images of the S-A (a) and S-B (b) and the size distribution analysis of them measured by Nano Measurer 1.2

The effects of some hydrothermal reaction conditions on improving the fluorescence of the S-A were investigated. Experimental conditions are shown in Table 1.

Table 1. Hydrothermal Reaction Conditions*

Entry	S-A (mL)	Amount of NaOH (mg)	Time (h)
1	2	60	6
2	2	60	8
3	2	60	10
4	2	0	10
5	2	40	10
6	2	60	10
7	2	80	10
8	2	120	10
9	1	114	8
10	2	114	8
11	3	114	8
12	4	114	8
13	5	114	8

* For each entry, the whole system was adjusted to 10 mL by addition of water, the reaction temperature was 200 °C

Figure 6a shows the effect of the hydrothermal time on enhancing the photoluminescence intensity (PL intensity) of the S-A, which was the maximum emission spectra at 420 nm under 330 nm excitation wavelengths (Entry 1-3). It could be seen that 8-10 h of hydrothermal time was sufficient to improve the PL intensity, and continuing to extend the time would not improve it significantly. Figure 6b shows the effect of amount of NaOH. In the case of 2 mL of the S-A and 10 h of reaction time (Entry 4-8), it was found that in the absence of NaOH (Entry 4), the PL intensity of the S-B was only changed from 4.4 to 52.5 arbitrary unit (a.u.). When 80 mg of NaOH (Entry 7) was used, the maximum PL intensity (194 a.u.) of the S-B was achieved. Excessive amounts of NaOH (Entry 8) did not improve the PL intensity of the S-A. Figure 6c shows the effect of the concentration of the original solution. When hydrothermal time was fixed at 8 h and the amount of NaOH was 114 mg (Entry 9-13), the PL intensity of the S-B reached its maximum value at a ratio of 114 mg of NaOH to 3 mL of the S-A (Entry 11). This result was consistent with the results from Entry 4-8, which revealed that the most appropriate ratio of NaOH to the amount of the S-A was 38-40 mg of NaOH to 1 mL of the S-A.

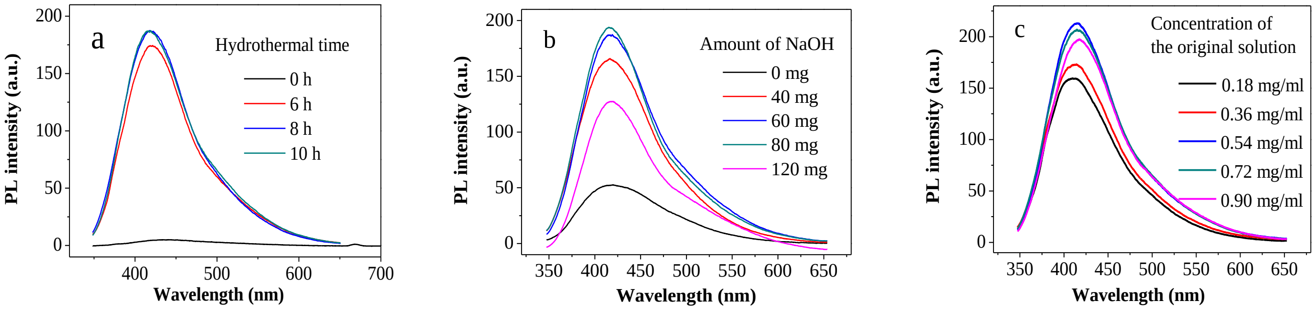

Fig. 6. Effects of hydrothermal time, amount of NaOH, and the concentration of the original solution on the PL intensity. (a) 2 mL of the S-A, 8 mL of water, and 60 mg of NaOH were sealed into a typical PTFE-lined autoclave system and hydrothermally reacted in a pre-heated oven at 200 °C for 0 h, 6 h, 8 h, and 10 h, respectively. (b) The hydrothermal time was fixed at 10 h, the usage of the S-A was 2 mL, water was 8 mL, and the reaction temperature was 200 °C. The amount of NaOH was 0 mg, 40 mg, 60 mg, 80 mg, and 120 mg, respectively. (c) The hydrothermal time was fixed at 8 h and the amount of NaOH was 114 mg; the amount of the S-A was 1 mL, 2 mL, 3 mL, 4 mL, and 5 mL, respectively. The whole system was adjusted to 10 mL by addition of water. The reaction temperature was 200 °C.

The detailed mechanism for the formation of the S-B was still not clear, but it was completely different from the case of improving photoluminescence of natural gas soot using the hydrothermal method (Tian *et al*. 2010), in which quinone moieties were effectively removed. Combining the observations of the UV-vis spectra and the XPS analysis of the S-A and S-B, the following speculations were suggested (Fig. 7): (1) The S-A was composed of tiny carbon particles with rich hydroxyl groups and a small amount of carbonyl groups and carboxyl groups. Due to their high O/C (0.63) atomic ratio, the S-A could be regarded as carbon particles composed of partial carbonized oligosaccharides. (2) These oligosaccharides were hydrolyzed to monosaccharides, followed by isomerization and dehydration to form 5-hydroxy furan aldehyde (Leshkov *et al*. 2006; Antal and Mok 1990), and further polymerized, producing C=C double bonds and conjugated structures under the alkaline hydrothermal conditions at 200 °C for 8 to 10 h. (3) The resulting aldehydes groups were disproportionated into carboxyl groups and hydroxyl groups at the hydrothermal high temperature and high pressure simultaneously. This resulted in the decrease of the atomic ratio of O/C (0.363) and the increase of the relative ratio of carboxyl groups of the S-B. It was the formation of the C=C double bonds and conjugated structures that promoted the ultraviolet absorptions and improved the fluorescence of the S-B.

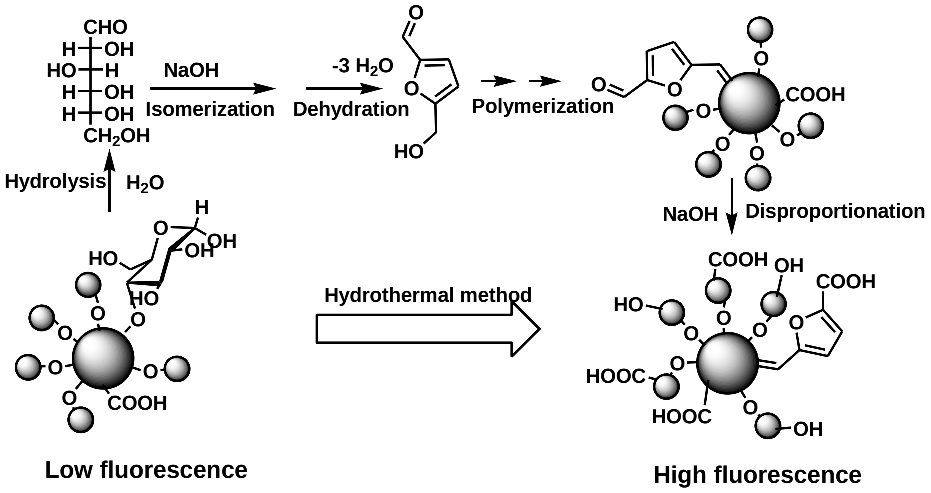

Fig. 7. The mechanism for the transformation from low fluorescence of S-A to high luminescence of S-B

CONCLUSIONS

From the above results, we can conclude that a weak fluorescent solution was obtained from the reflux system of the bagasse-based carbonaceous blocks and an aqueous solution of NaOH. The fluorescent properties of this solution were significantly improved under alkaline hydrothermal conditions. The hydrothermal process involves hydrolysis, isomerization, dehydration, and polymerization of the tiny carbon particles, causing the formation of the C=C double bonds and conjugated structures. The method of fabricating luminescent CDs by hydrothermal treatment under alkaline conditions is helpful for the production of luminescent nano-materials.

ACKNOWLEDGMENTS

We thank Tianjin Polytechnic University for the finance support.

REFERENCES CITED

Antal, M. J., and Mok, W. S. L. (1990). "Mechanism of formation of 5-(hydroxymethyl)-2-furaldehyde from d-fructose and sucrose," *Carbohydr. Res*. 199(1), 91-109.

Bourlinos, A. B., Stassinopoulos, A., and Anglos, D. (2008). "Photoluminescent carbogenic dots," *Chem. Mater*. 20, 4539-4541.

Bourlinos, A. B., Zboril, R., and Petr, J. (2012). "Luminescent surface quaternized carbon dots," *Chem. Mater*. 24(1), 6-8.

Dong, Y. Q., Zhou, N. N., and Lin, X. M. (2010). "Extraction of electrochemiluminescent oxidized carbon quantum dots from activated carbon," *Chem. Mater*. 22(21), 5895-5899.

Fu, C. C., Lee, H. Y., and Chen, K. (2007). "Characterization and application of single fluorescent nanodiamonds as cellular biomarkers," *Proc. Natl. Acad. Sci. U. S. A*. 104, 727-732.

Hu, S. L., Niu, K. Y., and Sun, J. (2009). "One-step synthesis of fluorescent carbon nanoparticles by laser irradiation," *J. Mater. Chem*. 19, 484-488.

Kaczmarek, H., and Czerwinski, W. (2002). "The influence of polychromatic UV-irradiation on new thiophene copolymers," *J. Photochem. Photobiol. A*146(3), 207-218.

Lakowicz, J. R. (1999). *Principles of Fluorescence Spectroscopy*, 2nd Ed, Kluwer Academic / Plenum, New York.

Leshkov, Y. R., Chheda, J. N., and Dumesic, J. A. (2006). "Phase modifiers promote efficient production of hydroxymethylfurfural from fructose," *Sci*. 312, 1933-1937.

Liu, H. P., Ye, T., and Mao, C. D. (2007). "Fluorescent carbon nanoparticles derived from candle soot," *Angew. Chem. Int. Ed*. 46, 6473-6475.

Liu, R. L., Wu, D. Q., and Liu, S. H. (2009). "An aqueous route to multicolor photoluminescent carbon dots using silica spheres as carriers," *Angew. Chem. Int. Ed*. 121(25), 4668-4671.

Pan, D. Y., Zhang, J. C., and Li, Z. (2010). "Hydrothermal route for cutting graphene sheets into blue-luminescent graphene quantum dots," *Adv. Mater*. 22(6), 734-738.

Peng, H., and Travas-Sejdic, J. (2009). "Simple aqueous solution route to luminescent carbogenic dots from carbohydrates," *Chem. Mater*. 21, 5563-5565.

Ray, S. C., Saha, A., and Jana, N. R. (2009). "Fluorescent carbon nanoparticle: Synthesis, characterization and bio-imaging application," *Phys. Chem. C* 113(43), 18546-18551.

Sun, Y. P., Zhou, B., and Lin, Y. (2006). "Quantum-sized carbon dots for bright and colorful photoluminescence," *J. Am. Chem. Soc*. 128, 7756-7757.

Tian, L., Ghosh, D., and Chen, W. (2009). "Nanosized carbon particles from natural gas soot," *Chem. Mater*. 21, 2803-2809.

Tian, L., Song, Y., and Chang, X. (2010). "Hydrothermally enhanced photoluminescence of carbon nanoparticles," *Scripta. Mater*. 62, 883-886.

Yu, S. J., Kang, M. W., and Chang, H. C. (2005). "Bright fluorescent nanodiamonds: No photobleaching and low cytotoxicity," *J. Am. Chem. Soc*. 127, 17604-17605.

Zhang, J., Shen, W., and Pan, D. (2010). "Controlled synthesis of green and blue luminescent carbon nanoparticles with high yields by the carbonization of sucrose," *New J. Chem*. 34, 591-593.

Zhao, Q. L., Zhang, Z. L., and Huang, B. H. (2008). "Facile preparation of low cytotoxicity fluorescent carbon nanocrystals by electrooxidation of graphite," *Chem. Commun*. 41, 5116-5118.

Zheng, L.Y., Chi, Y. W., and Dong, Y. Q. (2009). "Electrochemiluminescence of water-soluble carbon nanocrystals released electrochemically from graphite," *J. Am. Chem. Soc*. 131, 4564-4565.

Zhou, J., Booker, C., and Li, R. (2007). "An electrochemical avenue to blue luminescent nanocrystals from multiwalled carbon nanotubes (MWCNTs)," *J. Am. Chem. Soc*. 129, 744-745.

Zhou, J. H., Sui, Z. J., and Zhu, J. (2007). "Characterization of surface oxygen complexes on carbon nanofibers by TPD, XPS and FT-IR," *Carbon* 45(4), 785-796.

Zhu, H., Wang, X., and Li, Y. (2009). "Microwave synthesis of fluorescent carbon nanoparticles with electrochemiluminescence properties," *Chem.Commun*. 34, 5118-5120.

APPENDIX

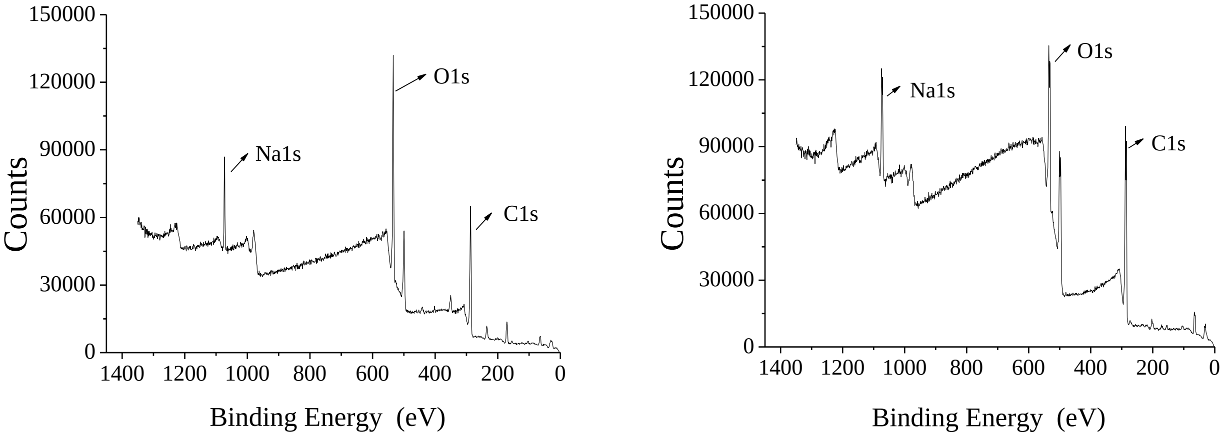

(a) (b)

Figure S1. XPS analysis of the S-A (a) and S-B (b)

Article submitted: January 8, 2013; Peer review completed: February 10, 2013; Revised version received and accepted: March 29, 2013; Published: April 3, 2013.